General Disclaimer

One or more of the Following Statements may affect this Document

- This document has been reproduced from the best copy furnished by the organizational source. It is being released in the interest of making available as much information as possible.

- This document may contain data, which exceeds the sheet parameters. It was furnished in this condition by the organizational source and is the best copy available.

- This document may contain tone-on-tone or color graphs, charts and/or pictures, which have been reproduced in black and white.

- This document is paginated as submitted by the original source.

- Portions of this document are not fully legible due to the historical nature of some of the material. However, it is the best reproduction available from the original submission.

NASA Technical Memorandum 78819

MEASUREMENTS OF ACOUSTIC SOURCES IN MOTION

L. MAESTRELLO AND T. D. NORUM

DECEMBER 1978

NASA
National Aeronautics and Space Administration
Langley Research Center
Hampton, Virginia 23665

MEASUREMENTS OF ACOUSTIC SOURCES IN MOTION

by

L. Maestrello and T. D. Norum
NASA Langley Research Center
Hampton, Virginia 23665

SUMMARY

This report presents results of the far-field pressures measured from three different types of moving sources. These acoustic sources consist of a point monopole, a small model jet, and an aircraft. Results for the pressure time history produced by the point source show good agreement with those predicted analytically. Both actual and simulated forward motion of the model jet show reductions in noise levels with forward speed at all angles between the source and observer. Measurement with the aircraft over both an anechoic floor and over the ground yields a method for evaluating the transfer function for ground reflections at various angles between the moving aircraft and measurement position.

INTRODUCTION

This report discusses three types of experiments on moving noise sources and the interpretation of the measured far-field pressures. The experiments consist of i) a point source moving above a finite impedance reflecting plane, ii) a model jet in actual and simulated forward motion, and iii) an airplane flyover with and without ground reflection effects. This work is an integral part of a prediction scheme for the effects of forward motion on noise radiation. From the practical point of view, one must account for the effects of motion of the sources and their location relative to nearby scattering surfaces.

In section I, preliminary information on the motion of noise sources is obtained by looking at the simplest source, the point monople (Ref. 1). The experiment is carried out using a small monochromatic source which behaves like an acoustic monopole when stationary. The purpose of this experiment is to determine the behavior of the source when in motion at constant speed.

There are different types of sources that radiate in the same manner in a stationary medium but radiate differently when in motion. The present experimental source consists of a time rate of introduction of mass, so it should behave like an acoustic monopole in the wave equation for the velocity potential. The experiment was designed to determine if motion yields the expected changes in source directivity.

The source was positioned above an automobile via a guy wire supported mast. The automobile was driven at constant speeds over an asphalt surface past a stationary microphone. The resulting measured time histories were then compared to analytical computations of a monopole moving above a finite impedance reflecting plane.

Section II reports experiments of a model jet in both actual and simulated motion (Ref. 2). The model nozzle was first mounted above the same automobile used in the experiments reported above. The vehicle was again driven past stationary microphones in order to quantify the effects of motion on jet mixing noise. The nozzle was then tested in an anechoic environment with a free jet simulating the forward motion. The results of these two methods of obtaining forward speed effects on jet noise are compared.

In section III, tests conducted using an airplane (a T-38 NASA trainer vehicle) are reported. Measurements were taken over an anechoic floor as well as over the ground, and auto-correlations of these measurements were obtained for short time intervals corresponding to a particular position of the aircraft. These show the direct signal for the microphone over the anechoic floor as well as a combination of the direct and reflected signals for the microphone above the ground.

The simultaneous processing of the signals received by the two microphones permits one to determine the transfer function of the surface for a large range of frequencies and source positions. This approach will permit correction of flyover spectra for contamination by ground reflections.

The results of these three tests are presented and discussed together with recommendations for future work.

I. POINT SOURCE IN MOTION

The experiment was conducted by placing a point source above an automobile, and driving it over an asphalt surface past sideline microphones. An analysis for an acoustic monopole moving above a reflecting plane was made and results from the experiment and analysis are compared for different forward speeds.

A. Description of Experiment

The experimental source consisted of a 60 watt acoustic driver necked down to a 1.52 cm diameter tubular opening. When driven by an oscillator at a discrete frequency, the output of this source consists of tones at the oscillator frequency and its harmonics. By appropriate filtering, the measured signal consists essentially of a discrete frequency.

The source was positioned 7.9 m from the ground above an automobile via a guy wire supported mast (Fig. 1). An oscillator located in the trunk of the vehicle excited the source at a frequency of either 1230 Hz or 2310 Hz. The automobile was driven at constant speeds ranging from 13.4 to 44.7 m/z which were recorded on a strip chart within the vehicle. Sideline microphones were located at a closer approach distance of 11.0 m and positioned 3.05 m and 6.10 meters from the ground surface. The experiment was performed on an aircraft runway consisting of a 16.5 cm asphalt surface on top of a concrete foundation.

Figure 1.- Moving point source experiment.

The pressure signals were measured with 1.3 cm diameter condenser microphones and recorded on magnetic tape. In both the recording and reproduction stages the data were passed through a band pass filter set to pass all the frequency components possible due to the Doppler effect on the oscillator frequency. The analog tapes were digitized at the rate of 10,000 points per second.

The oscillator frequency was set to an accuracy of $\pm$ 1 Hz. Vehicle speed varied by no more than $\pm$ 0.5 m/s over the test zone. The frequency response of the recording and analysis system was estimated to be flat within $\pm$ 0.5 dB over all frequencies of interest.

B. Analysis

For the monopole of angular frequency ω and strength q_0 moving with constant velocity U in the x direction at a distance h above the x-z plane (Fig. 2), the propagation is governed by:

$$\Box^2 \psi (x, y, z, t) = - q_0 e^{-i\omega t} \delta(x-Ut) \delta(y-h) \delta(z) \tag{1}$$

where $\Box^2$ is the wave operator, $\nabla^2 - \frac{1}{c^2} \frac{\partial^2}{\partial t^2}$, and ψ is the acoustic velocity potential. Specifying the x-z plane to be a locally reacting surface of normal impedance ζ, the velocity potential must satisfy the condition:

$$\frac{1}{c} \frac{\partial}{\partial t} - Z \frac{\partial}{\partial y} \psi(x, y, z, t) = 0 \quad \text{at} \quad y = 0 \tag{2}$$

where $Z = \zeta/\rho c$ and ρc is the acoustic impedance of air.

Through the use of a Lorentz transformation and a subsequent Fourier transformation on the spatial variables, the solution valid at a sufficient distance above the plane is

$$\psi(x, y, z, t) \cong (q_0/4\pi)\, e^{ik\gamma^2(ct-Mx)} \left(e^{ik\gamma^2 R_1}/R_1 + C_R\, e^{ik\gamma^2 R_2}/R_2\right), \tag{3}$$

where

$$R_1 = [(x - Mct)^2 + ((y - h)/\gamma)^2 + (z/\gamma)^2]^{1/2}, \tag{4a}$$

$$R_2 = [(x - Mct)^2 + ((y + h)/\gamma)^2 + (z/\gamma)^2]^{1/2}, \tag{4b}$$

$$C_R = \frac{Z(y + h) - \gamma^2(R_2 + M(x - Mct))}{Z(y + h) + \gamma^2(R_2 + M(x - Mct))} . \tag{4c}$$

Note that if the Mach number M is set equal to zero the solution reduces to that for the stationary source (Ref. 3) with the reflection coefficient given by

$$C_R = (Z \cos\alpha - 1)/(Z \cos\alpha + 1), \tag{5}$$

where $\alpha = \cos^{-1}[(y + h)/(x^2 + (y + h)^2 + z^2)^{1/2}]$ is the angle of incidence. This stationary source solution is stated in reference 3 to be a very good approximation as long as the observer is not closer than a half-wavelength to the boundary surface.

Hence, in addition to the well-known convection effects on the form of the direct and reflected waves, source motion introduces a convection term into the reflection coefficient. This convection term in Eq. (4c) is seen to be more important for small values of impedance and large incidence angles (small grazing angles), and increases in significance as the source velocity increases.

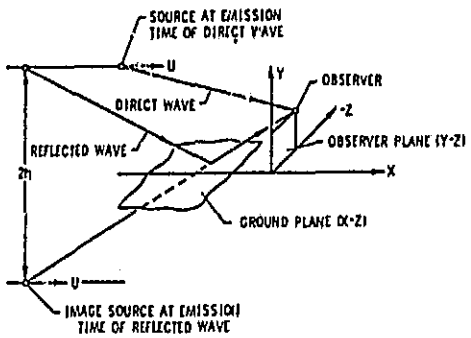

Figure 2.- Source moving at constant velocity above a ground plane.

The acoustic pressure is obtained in the usual manner from the velocity potential by

$$p(x, y, z, t) = - \rho \partial \psi(x, y, z, t)/\partial t. \qquad (6)$$

C. Results and Comparisons

To investigate the effects of motion on the experimental point source and the extent to which the observed signal can be predicted analytically, various comparisons of the time histories were made. These comparisons are shown in figures 3-5, in which the mean square pressure in dB is plotted against the normalized time Ut/σ, where U is the source velocity and σ is the closest approach distance. The analytical mean square pressure was computed at discrete points in time from Eq. (6), whereas the experimental values were obtained by averaging the digitized data over a time interval corresponding to a given increment in the source travel distance. The comparisons below include the effect of analysis time on the perceived results and the effects of varying source velocity and observer height.

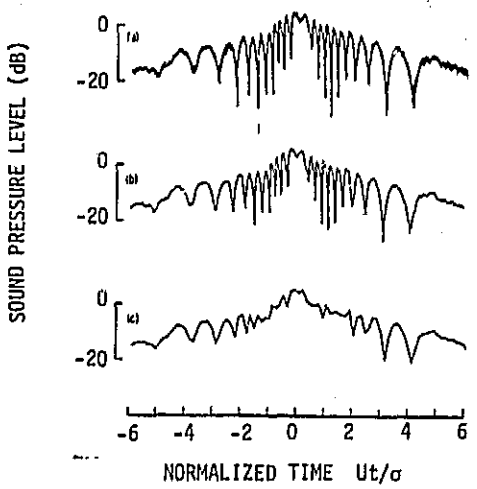

Figure 3.- Effect of analysis time on experimental noise-time history. Source frequency F = 1230 Hz; source velocity U = 13.4 m/z; observer height h = 3.05 m; analysis time: (a) 1.52 cm/point, (b) 10.7 cm/point, (c) 152 cm/point

To see the effect of analysis time on the observed signal, one of the experimental time histories was analyzed using three different analysis times. In figure 3a, each plotted point corresponds to 1.52 cm of source travel distance (1.52 cm/point), whereas 10.7 cm/point and 152 cm/point were used in figure 3b and 3c, respectively. Each of the first two curves show the pattern of alternate reinforcements and cancellations caused by the reflected wave, although the magnitudes of the cancellations are seen to differ by as much as 10 dB between the two curves. (The same phenomena was obtainable with the theoretical results when different time intervals between computed points were used.) This not unexpected fact illustrates that little information about the reflected wave from an acoustically hard surface can be obtained from a consideration of the magnitude of the cancellations. Figure 3c shows that the details of the reflection process are lost if the analysis time is not chosen small enough.

A comparison of the theoretical and experimental results is given in figure 4 for the two different observer heights. The time interval between computed points for all the theoretical curves presented was chosen to correspond to 10.7 cm/point. Superimposed on each of these curves is the signal that would be received in the absence ofthe ground surface, obtained by using a value of zero for the reflection coefficient. The value chosen for the normalized ground impedance in the theoretical curves was $Z = 4 - i4$, a value indicative of a fairly hard ground surface. One can see a good agreement between the curves both in shape and in the time intervals between the alternate reinforcements and cancellations. Decreases in the time interval between successive reinforcements and cancellations are seen to occur in both the theoretical and experimental results with increasing ground to observer distance.

The effect of source velocity can be seen in figure 5. Since the time axis has been normalized by using the velocity, the shapes of the observed signal are the same. (The erratic nature of the experimental curves with increasing velocity is due to a smaller analysis time being used as the velocity increases.)

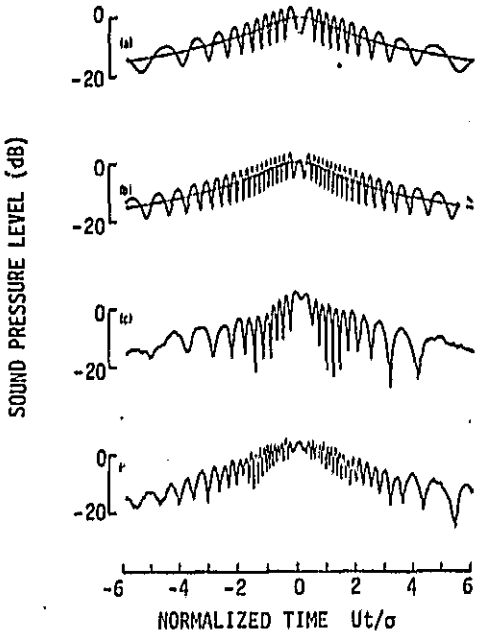

Figure 4.- Variation of theoretical and experimental noise-time histories with observer height. Source frequency F = 1230 Hz; source velocity U = 13.4 m/s; impedance Z for computed curves = 4 - i4; observer height h: (a) 3.05 m (computed); (b) 6.10 m (computed); (c) 3.05 m (measured); (d) 6.10 m (measured).

Many of the above results are qualitatively predictable from a simple consideration of the time and length scales involved. The purpose of the comparisons presented is to show the good agreement in the shapes of the experimental and theoretical results. This agreement gives credance to the assumption that the experimental source indeed radiates in the same manner as a theoretical monopole in motion.

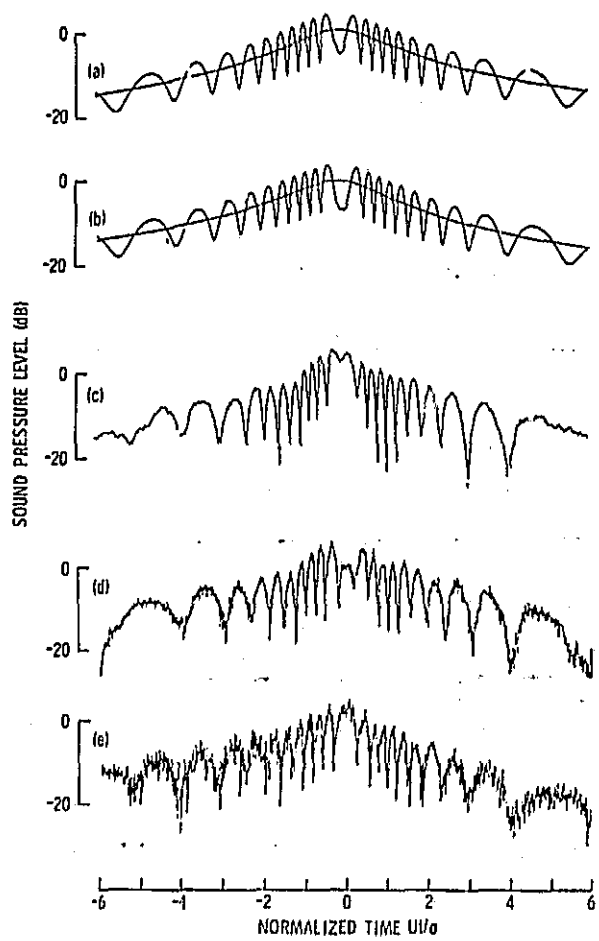

Figure 5.- Variation of theoretical and experimental noise-time histories with source velocity. Source frequency F = 1230 Hz; observer height h = 3.05 m; impedance Z for computed curves = 4 - i4; source velocity U: (a) 13.4 m/s (computed); (b) 35.7 m/s (computed); (c) 13.4 m/s (measured); (d) 22.3 m/s (measured); (e) 35.7 m/s (measured).

II. MODEL JET IN ACTUAL AND SIMULATED MOTION

The model nozzle was mounted above the automobile in the same manner as the point source and driven past fixed microphones. The nozzle was then mounted in a anechoic facility inside a large free jet simulating the forward motion. These two methods of obtaining forward speed effects on jet mixing noise are compared.

A. Tests with the Vehicle

The noise generated by the automobile in motion was estimated from the test discussed in section I. Since the vehicle noise is predominantly low frequency, a high pass filter can be used to suppress much of this background noise. This necessitates the use of a high speed, small diameter jet to maintain the spectral peak of the jet noise above the low frequency cutoff. Hence a 2.54 cm exit diameter nozzle run at a nominal Mach number of 0.85 was chosen along with a 500 Hz high pass filter. Since the spectral peak of jet noise corresponds to a Strouhal number near 0.25, this peak should then occur around 3 kHz.

A more obvious reason for the high jet exit velocity was to obtain jet noise levels above that of the vehicle noise throughout most of the spectra. Also, the high jet levels assured minimum contamination from upstream valve noise.

The nozzle flow was provided by a high flow accumulator filled with nitrogen and mounted in the trunk of the vehicle. The gas passed through a long supply tube to the nozzle exit. For the chosen exit Mach number of 0.85, between 2 and 3 seconds of constant mass flow could be obtained from this system.

Both the nozzle and microphones were positioned approximately 7.6 m (25 ft.) above the ground and the closest approach distance between vehicle and microphones was about 11 m.

The test vehicle was driven over an asphalt surface past six sideline microphones at a constant speed within the test section. The microphones were positioned at 3 m intervals parallel to the path of the vehicle. Since the nozzle supply system was limited to about 2.5 seconds, measurements at all angles of interest could not be obtained during a single run. Hence each run was set up to obtain data for a single nozzle to microphone emission angle. The vehicle position with respect to the microphones was determined by long metal strips that functioned as electrical switches. These were placed perpendicular to the path of the vehicle and activated by its tires. The signals produced by these switches were recorded along with the microphone signals. Each microphone signal was analyzed only over 3 m of vehicle motion such that the midpoint of the signal corresponded to the desired nozzle-microphone angle at the emission time. Vehicle background noise was measured using the same procedure without the jet activated.

Static jet noise data at each emission angle were obtained from two of the six microphones, with the stationary vehicle positioned such that the two microphones were located at the extreme angles of the corresponding motion run.

Five discrete nozzle-microphone emission angles were tested, equally spaced from 30^0 to 150^0. Vehicle Mach numbers of 0, 0.04, 0.08, and 0.12 were run at all five angles, with the exception that data were not obtained at the two upstream angles at the highest speed due to a significant masking of the jet signal by the vehicle noise. Each test condition (corresponding to a given vehicle speed and angle) was repeated a number of times, resulting in at least 2 seconds of data per condition.

Power spectral densities (PSD's) were obtained from the measurements using a constant bandwidth filter of 78 Hz over the range 500 Hz to 20 kHz. Each acceptable data segment was analyzed and those corresponding to a given test condition averaged.

The PSD's for all test conditions at a nozzle-microphone angle of 30^0 are shown in figure 6. The background vehicle noise (jet-off condition) is shown as the continuous traces in the lower part of the figure. Data at the highest speed in the frequency region near 4.5 kHz are not shown since this region was contaminated by background noise due to aeolian tones caused by the guy wires supporting the nozzle supply tube.

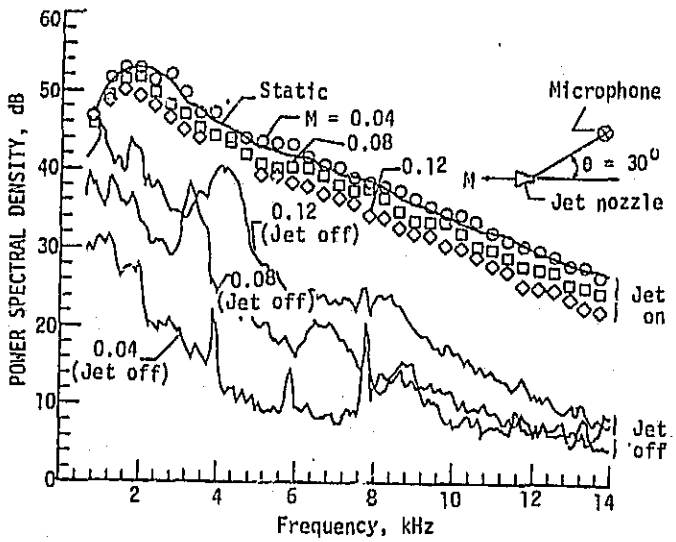

Figure 6.- Measured power spectral densities for jet and vehicle noise at 30^0 emission angle.

There is no discernable difference between the static and motion spectrum at the lowest vehicle speed. At the higher speeds, however, a level difference can be noticed over almost the entire spectrum, this difference increasing as the vehicle speed is increased. Also noted is the expected Doppler shift of the peak frequency to lower values with increasing speed.

This decrease in level across the spectrum with increasing forward speed was obtained at all angles. Details of these results can be found in reference 2.

Since portions of the measured PSD's were contaminated by background noise, the overall sound pressure levels (OASPL) were estimated from the uncontaminated portions of the spectra. The estimated OASPL's are shown in figure 7 along with the results computed from the contaminated PSD's. It can be seen that there is a consistent decrease in the estimated OASPL with increasing forward velocity at all nozzle-microphone emission angles, as one would expect from the spectral results mentioned above.

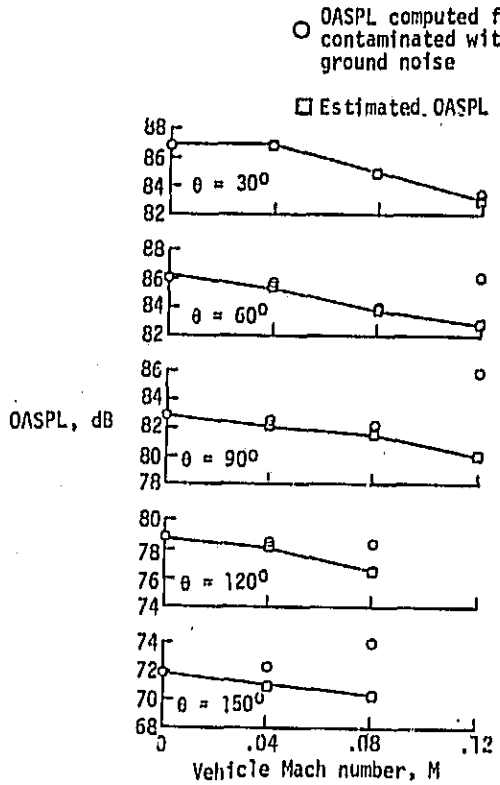

Figure 7.- Variation of overall sound pressure level with forward velocity. (Moving vehicle tests.)

B. Tests with the free jet

The free jet used to simulate forward motion was limited to a maximum Mach number of 0.11. Positioning of the jet in the anechoic chamber restricted measurements in the upstream direction to 120°. Other than these limitations, test conditions with the vehicle were repeated using the free jet. Air was used instead of pure nitrogen for the model jet.

The free jet exhausted vertically from a 1.2 m diameter nozzle into an anechoic environment. The 2.5 cm jet nozzle was positioned at the center of the free jet. A 1.3 cm (half-inch) condenser microphone designed for free-field linear response past 20 kHz was located on a boom that traversed an arc about the center of the model nozzle exit plane on a 3.7 m radius.

With the model jet maintained at a Mach number of 0.85 the free jet was run at the static case (no flow), and Mach numbers of 0.04, 0.08, and the maximum available, 0.11. For each test condition the microphone was held stationary at discrete angles from the downstream centerline ranging from 30° to 120°.

The noise generated above 500 Hz by the free jet was insignificant at all test conditions. Hence, the problems associated with background noise present in the vehicle tests were nonexistent during the tests with the free jet. However, the presence of the free jet shear layer requires corrections to correlate noise emission angle with observer angle.

Acoustic pressure power spectral density measurements using 400 Hz bandwidth are shown in figure 8 for the test conditions corresponding to an observer angle of 90°, the angle where the shear layer corrections are a minimum. One can make here the same observation as with the vehicle test-relative motion tends to decrease the jet noise level throughout the spectrum.

The true emission angles corresponding to the measured results were computed in the standard manner (c.f. ref. 4) under the assumption that the noise originates at the nozzle exit. (Amplitude corrections due to the shear layer were found to be less than 0.5 dB for all test conditions and hence were neglected.) The measured OASPL is given in figure 9 as a function of the computed emission angle. Again, a decrease in the OASPL is observed at all angles with increasing forward speed.

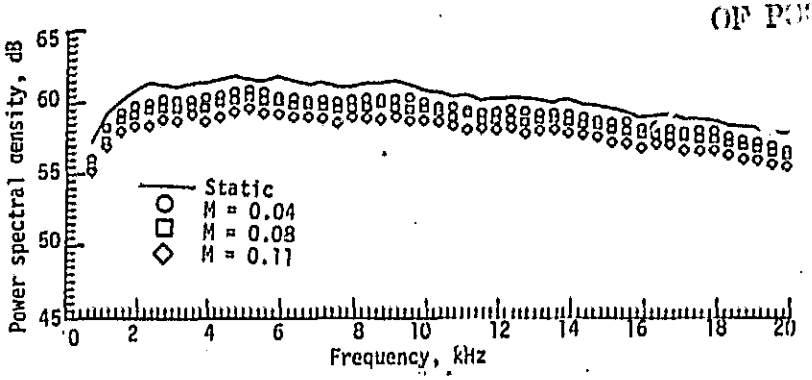

Figure 8.- Power spectral densities from free-jet at 90° observer angle.

C. Comparisons Between Vehicle and Free Jet Results

The difference in sound pressure level between static and motion conditions is generally correlated against the ratio of jet velocity to relative velocity (the difference between jet and forward velocities). This type of comparison should yield consistent results for flight simulation studies (free jet or wind tunnel) since there is no relative motion between the jet and the observer. However, in actual flight the Doppler effect results in a frequency shift of the entire spectrum, so this type of comparison (particularly when done on a frequency-by-frequency basis) can be misleading. Nevertheless, in order to reassert the main findings of this report in a fashion that is commonly presented, the static-to-motion OASPL differences are given in figure 10 as a function of 10 log M_J/M_{rel} for both series of tests. The effects due to convection that are sometimes subtracted from the OASPL differences before this type of correlation is made (ref. 4) were computed to be less than 0.4 dB for all test conditions and hence were neglected.

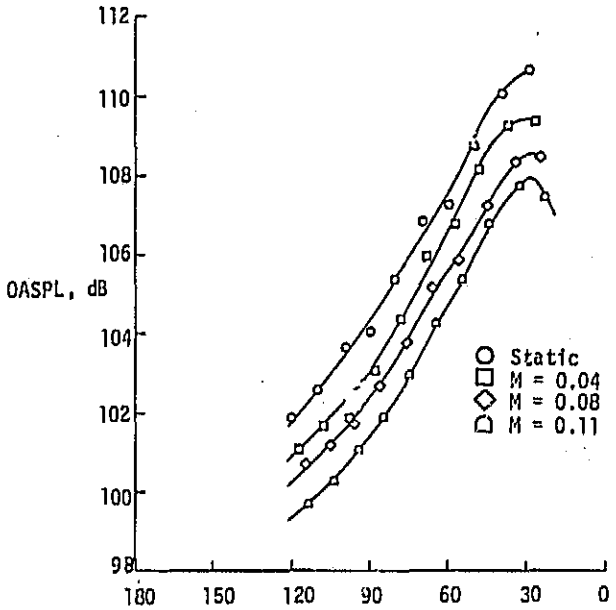

Figure 9.- Overall sound pressure levels including angular refraction correction. (Free-jet tests.)

The uncertainty due to the procedure used in estimating the OASPL for the vehicle tests leads to the considerable scatter shown in figure 10. The relative velocity exponent m lies somewhere between 3 and 6. The data uncertainty as well as the test limitations of high jet velocity/low forward speed prevent a reasonable estimate of this exponent or its variation with emission angle. Nevertheless, an increase in noise reduction with increasing forward speed is again clearly indicated at all angles at these low velocities for both testing methods.

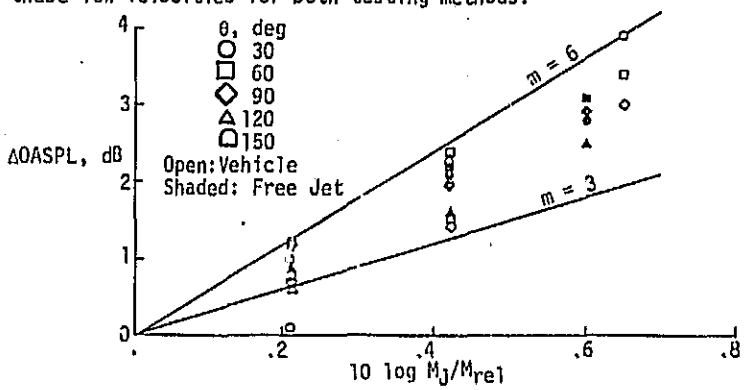

Figure 10.- Change in overall sound pressure level between static and motion conditions.

III. AIRCRAFT FLYOVER MEASUREMENTS

To better estimate the effect of forward motion on real engine noise, flight experiments were conducted using an actual aircraft. There are considerable difficulties to overcome before interpreting the far field data from a full scale aircraft in flight. Existing studies on forward flight have yet to address these difficulties but have concerned themselves with more obvious practical prerequisities. Since the results of aircraft flyovers are still dubious, it becomes important to establish exact techniques to quantize the sound field from a moving aircraft. This section focuses on one of the fundamental measurement problems, ground reflections. Measurements of the far field pressure from an airplane flyover were taken over both an anechoic floor and over the ground. A method is presented for evaluating the transfer function of the ground surface, which can be used for correcting data contaminated by ground reflections. These corrections are independent of the source, but depend on the geometrical orientation between the sources and observer as well as on the distance from the microphone to the ground surface.

A. Method of Measurements

Since the objectives of this test were to separate the effects of reflection and to establish the properties of the reflecting surface, microphones were located over both an anechoic floor and a reflecting ground. The anechoic floor is shown in Figure 11. It consists of a semicircular surface with a radius of 12.2 m composed of anechoic wedges of size 0.3 x 0.3 x 0.9 meters. The wedges are placed one meter above the ground and supported by wire mesh.

Four equally spaced microphones were placed over the anechoic floor, and an additional four over the ground (Fig. 12). The microphones were oriented along the direction of the flight path at a height of 3.38 m above the ground. The ground surface consists of packed turf, typical of surfaces used in aircraft flyover noise test. All the microphones are recorded simultaneously on magnetic tape recorder so that the measurements over the anechoic floor and over the ground surface were taken at the same time. The aircraft used was a NASA T-38 airplane (Fig. 13). One of the interesting features of this aircraft is that the two jets exhaust at the rear end of the fuselage, thus concentrating the emission over a small area. The test was conducted at an altitude of $h = 305$ meter at velocity of $V_f = 105$ m/sec.

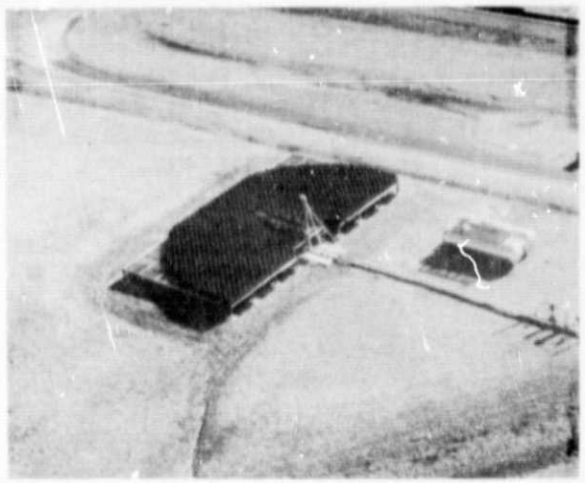

Figure 11.- Outdoor anechoic test facility

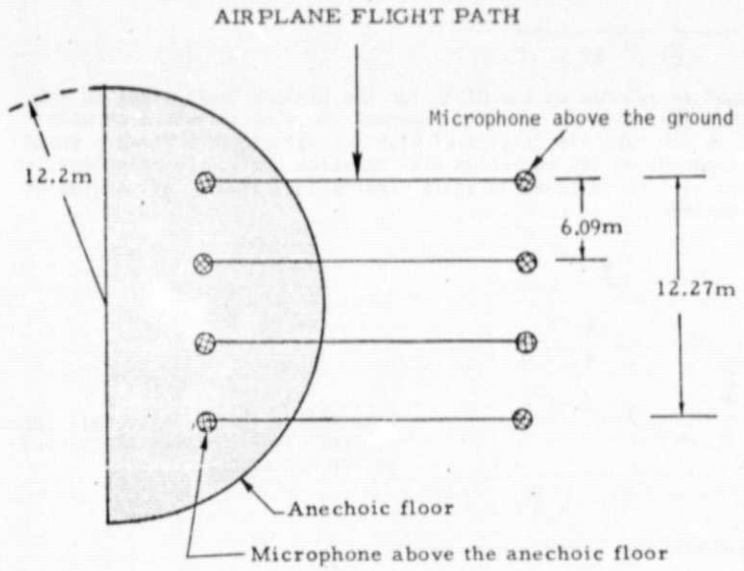

Figure 12.-Microphones positions above the anechoic floor and above the ground

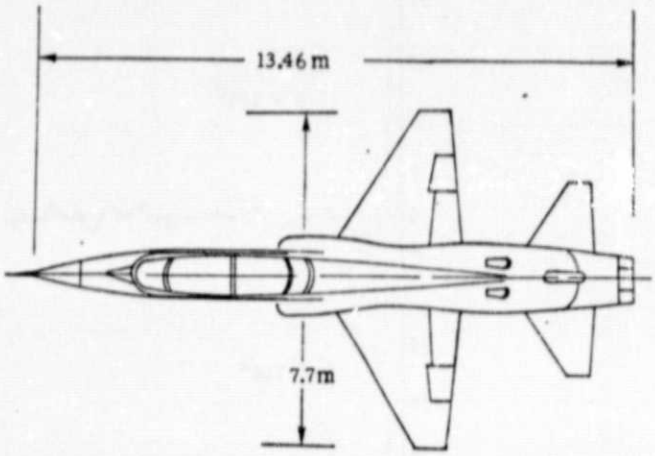

Figure 13.- Geometry of T-38 airplane

B. Results and Discussion

The data collected in one flyover was recorded over the time period of 14 seconds. During this time the aircraft moved over a 140^0 arc with respect to the reference microphone. Seven auto-correlations were obtained, each over one record time interval, centered at the angles $\theta = 36^0$, 55^0, 90^0, 124^0, 144^0, 156^0, and 160^0 (Fig. 14). The overhead position of the aircraft (90^0) is chosen as reference, such that at $\theta = 36^0$ the airplane is four seconds ahead of the reference, and at $\theta = 160^0$ is is eight seconds past the reference.

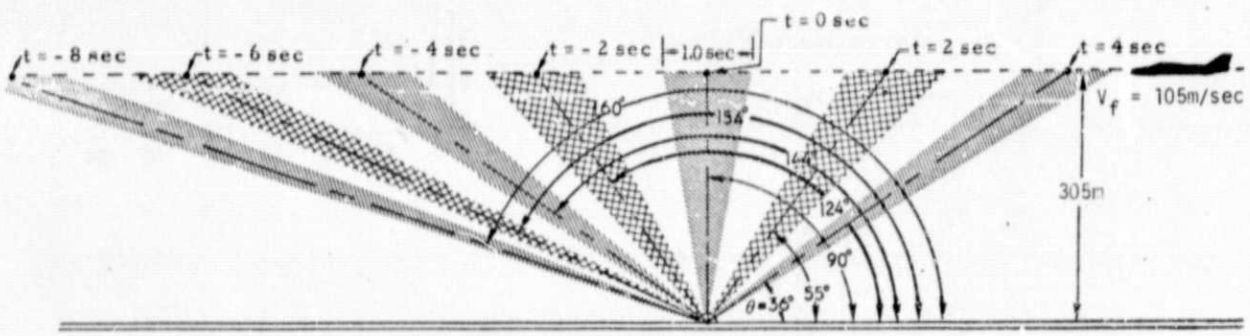

Figure 14.- Positions of the aircraft for data analysis

The auto-correlations taken over the anechoic floor are smooth while those taken over the ground contain a second peak (Figs. 15 and 16). The time delay of this peak depends on the position of the aircraft with respect to the microphone and is associated with the retarded time between the incident and reflected signals. At $\tau = o$, the auto-correlation measured over the ground consists of the direct signal and the reflected signal that was emitted at an earlier time, whereas the second peak at the time delay $\tau_o = \pm 2h \sin \theta/c$ consists of the correlation of the direct signal with itself after reflection.

In order to separately resolve the two peaks, the time delay of the secondary peak must be large in comparison with the correlation time scale of the direct signal. The measured signal can also be deconvoluted in the frequency domain, since the auto-correlation can be interpreted as the convolution of the transforms of both direct and reflected signals (See Ref. 4).

The position of the aircraft was determined from the auto-correlations over the ground. Notice that the time delays of the secondary peaks in Figure 16 increase from $\theta = 36^0$ to 90^0 and then decrease again as the angle becomes larger than 90^0, as expected from the expression relating τ_o to θ. Use of this expression along with the measured value of τ_o then yielded the aircraft postion (i.e., θ) at the emission time of the direct signal. In addition to using the auto-correlation to determine the position of the aircraft, the cross correlation between two adjacent microphones can also be used to estimate the speed of the aircraft.

The main objective of this experiment, however, is the evaluation of the transfer function (T) of the reflected signal from the surface. This function is defined as the ratio between the spectrum measured over the ground (S_g) to that measured over the anechoic floor (S_a) over the same time interval, and depends on the angle θ, the distance of the microphone from the ground (h), and frequency.

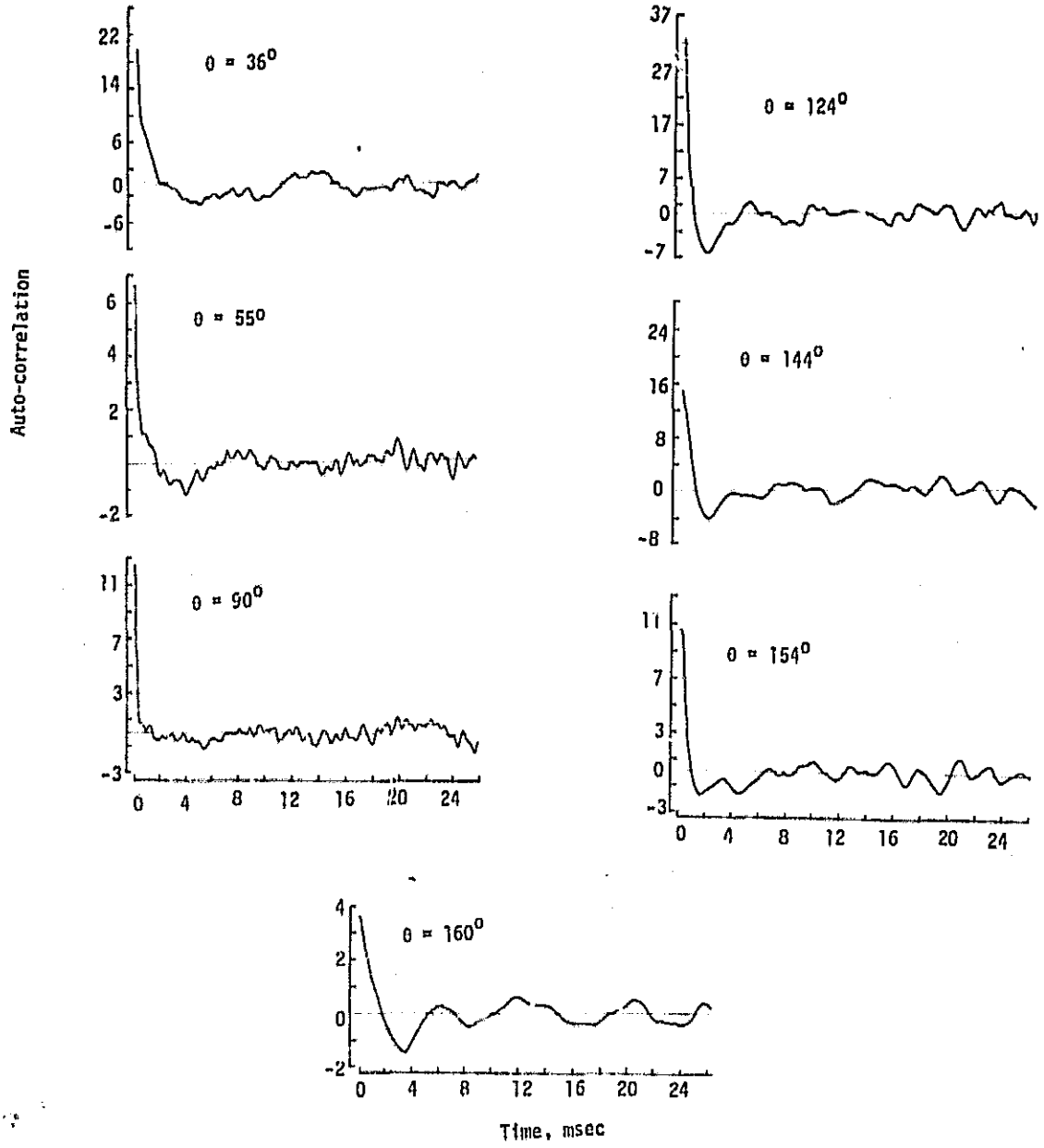

Figure 15.- Unnormalized auto-correlations over the anechoic floor.

Computed results of this transfer function are shown in Figure 17 for three different values of θ. The oscillatory behavior is due to the fact that the spectra from which the transfer function was derived are themselves not smooth because of the short averaging time necessitated by the motion of the source. Also, the nature of reflections leads to non-smooth spectra measured over the ground. However, for the practical purpose of correcting the ground spectrum for reflections, the transfer function can be averaged as shown by the smooth lines in Figure 17. These curves show that the corrections needed for ground reflections spread out in frequency as the source approaches the overhead position.

Using the average spectrum of the transfer function, the ground spectrum for $\theta = 36^{0}$ was corrected and shown in Figure 18 along with the two corresponding measured spectra. As can be seen from this figure, the spectrum corrected for ground reflections by the transfer function agrees well with the spectrum measured over the anechoic floor.

Pursuing ground reflection corrections utilizing the transfer function approach rather than the more common ground impedance measurements is certainly easier and more practical for any engineering approach. Measurements of surface impedance are known to be difficult and even at the present time these data are ambiguous and incomplete. In addition, discrete frequency measurements of surface impedance yields large scatter in results. The transfer function approach instead uses frequency bands so that oscillations are not as pronounced. Also, from the engineering approach it is easy to understand and simple to apply.

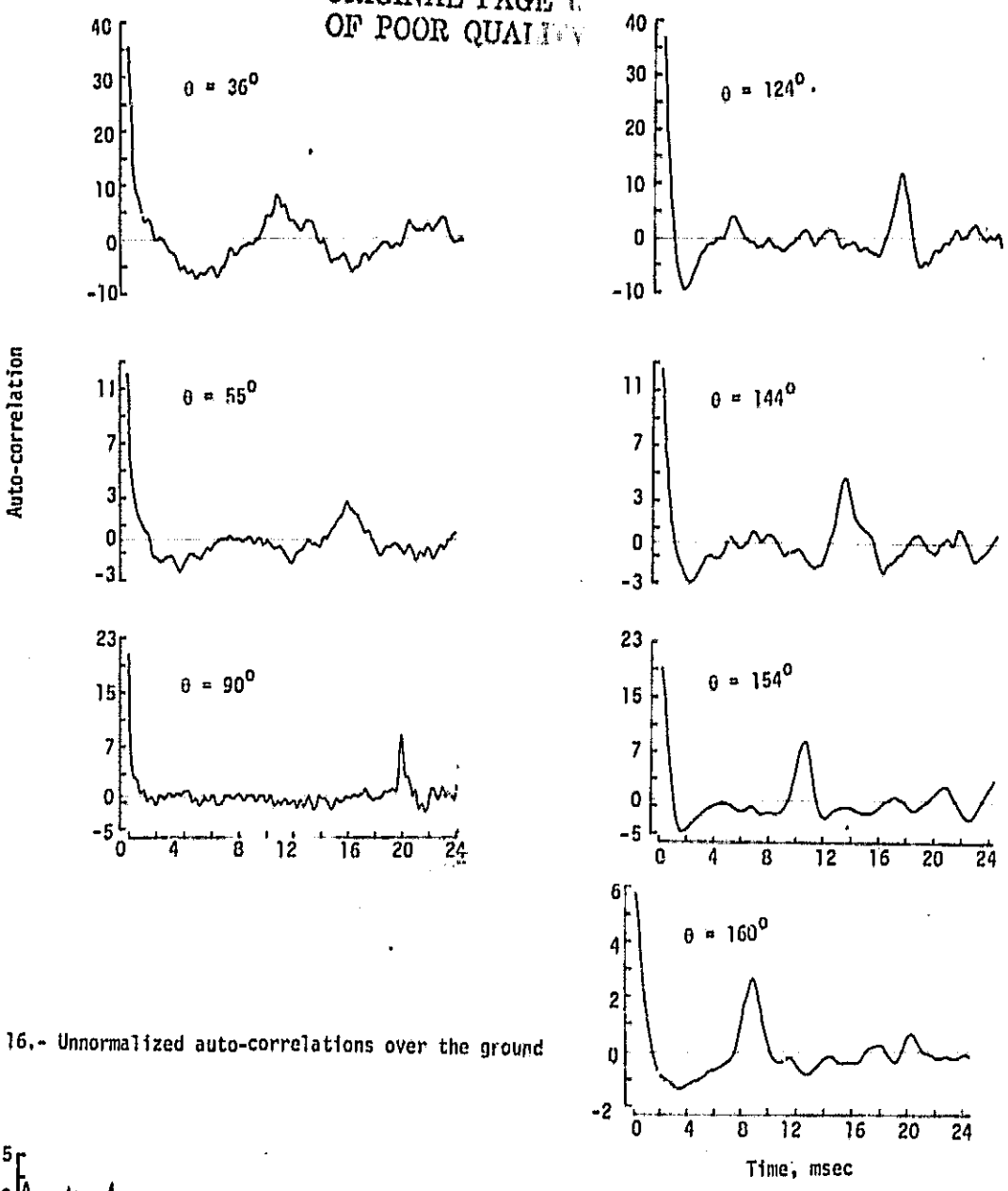

Figure 16.- Unnormalized auto-correlations over the ground

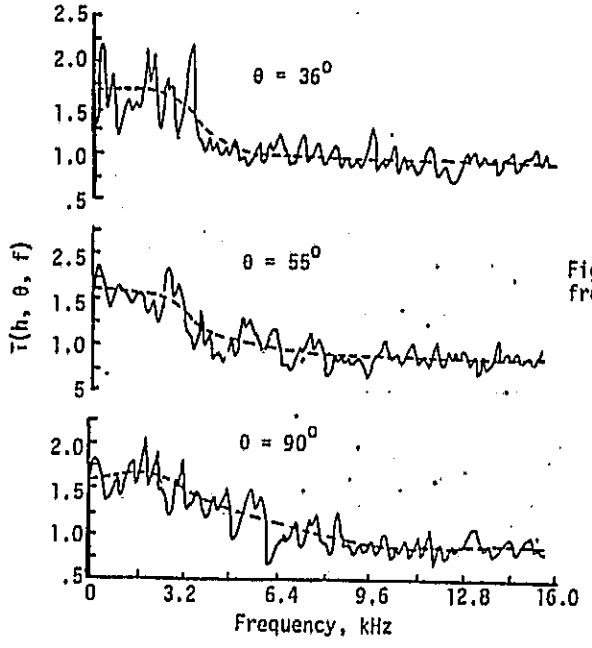

Figure 17.- Transfer function of the reflected signal from the surface of three different values of θ.

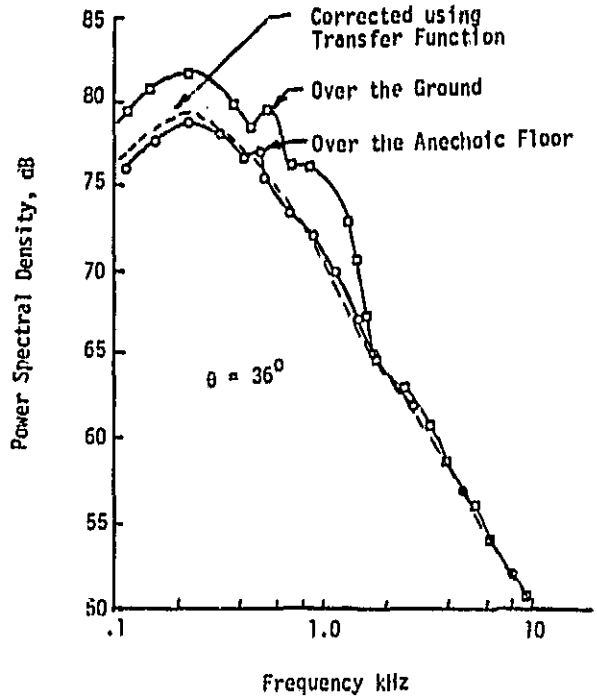

Figure 18.- Acoustic Spectra

CONCLUDING REMARKS

Experiments were conducted using three different types of noise sources in motion. A discrete frequency point source moving over a reflecting surface yields results that agree with those predicted analytically. Measurements of a model jet in actual and simulated forward motion both show that the noise decreases with increasing speed at all observation angles. The fact that observed effects in flight testing of actual jet engines do not appear in these model jet tests suggest that the flight data includes installation effects and, or sources other than pure jet mixing noise. Auto-correlations from noise measurements of an actual aircraft in flight over a ground surface gives an indication of reflections from the existence of a secondary peak in the correlation. This secondary peak also allows determination of the position of the aircraft. Simultaneous measurements over an anechoic floor and the ground permit the evaluation of the transfer function of the reflected signal from the surface and hence allow the spectrum to be corrected for ground reflections.

There is much work to be done to establish the effects of motion on aircraft noise. One step is the establishment of the temporal and spatial distribution of the sources in a jet in a fashion amenable to experimentation for both stationary and moving aircraft. This technique has been tested for a model stationary jet in reference 5. Furthermore, it is necessary to reduce the nonstationary signal (resulting from the motion of the aircraft) into an equivalent stationary one, such that comparison can be made between static and moving aircraft. A preliminary investigation of this effect is reported in reference 6.

REFERENCES

1. T. D. Norum and C. H. Liu, "Point Source Moving Above A Finite Impedance Reflecting Plane - Experimental and Theory," J. Acoust. Soc. Am. 63(4), April 1978.

2. T. D. Norum, "A Comparison of the Noise Produced By A Small Jet On A Moving Vehicle With That In A Free Jet." NASA T.P. 1326, December 1978.

3. R. K. Amiet, "Refraction of Sound By A Shear Layer," AIAA Paper 77-54, January 1977.

4. R. B. Rice, "Inverse Convolution Filters," Geophysics, Vol. 27, No. 1, 1962.

5. L. Maestrello and C. H. Liu, "Jet Noise Source Distribution from Far-Field Cross-Correlations," AIAA Journal, Vol 15, No. 6, June 1977.

6. E. McDaid and L. Maestrello, "The Estimation of Nonstationary Spectra From Moving Acoustic Source Distributions," AIAA Paper No. 72-667, June 1972.